Revision 1:
Accurate Determination of Ferric Iron in Garnets

[1]Ryan J. Quinn, [1]John W. Valley, [2]F. Zeb Page, [1]John H. Fournelle
[1] Dept. of Geoscience, University of Wisconsin, Madison, WI 53706
[2] Geology Department, Oberlin College, Oberlin, OH 44074

Abstract

Numerous techniques are available to determine the amount of Fe^{2+} and Fe^{3+} in minerals. Calculating Fe^{2+} and Fe^{3+} by charge-balance using electron probe microanalysis (EPMA) data is the most common method, but several studies question the usefulness and accuracy of this approach (McGuire et al., 1989; Dyar et al., 1993; Canil and O'Neill, 1996; Lalonde et al., 1998; Sobolev et al., 1999; Schmid et al., 2003; Li et al., 2005; Dyar et al., 2012; Schingaro et al., 2016). We compile and compare data for natural garnets that have been analyzed by both EPMA and Mössbauer spectroscopy. Comparison of $Fe^{3+}/\sum Fe$ determined by charge-balance vs. Mössbauer spectroscopy shows an approximate 1:1 correlation. The EPMA data set of Dyar et al. (2012) is reexamined and it is shown that disagreement between EPMA and Mössbauer for their data is not nearly as bad as reported. Data for charge-balance vs. Mössbauer spectroscopy are compared and show that the EPMA/charge-balance approach provides a suitable alternative when other methods are not practical.

Keywords: Ferric iron, EPMA, Charge balance, Mössbauer spectroscopy

Introduction

The oxidation state of iron is important to many aspects of mineralogy and petrology including thermobarometry and determination of oxygen fugacity in rocks or melts. Several methods exist for determining the ratio of Fe^{3+} to Fe^{2+}. Most commonly, it is either directly measured by wet chemistry (Wilson, 1960; Johnson and Maxwell, 1981) or Mössbauer spectroscopy (Dyar et al., 2006), or calculated from electron probe microanalysis (EPMA; e.g. Valley et al., 1983; Droop, 1987; Essene, 1989; Grew et al., 2013). Other techniques including X-ray photoelectron spectroscopy (Raeburn et al., 1997a, b), electron energy loss spectroscopy (Garvie and Buseck, 1998), EPMA-based 'flank method' (Höfer and Brey, 2007), and synchrotron based X-ray absorption near-edge spectroscopy (Bajt et al., 1994) have been employed to explicitly measure the valence of iron. The EPMA/charge-balance technique is the most frequently employed because of widespread EPMA accessibility, small spot size (~ 3 μm), and speed of analysis. Furthermore, analysis is essentially non-destructive. However, the EPMA/charge-balance approach is, in some circumstances, less precise and requires accurate analysis while making some assumptions: no vacancies, no unmeasured elements (e.g. H, Li, B), and that *Fe* is the only element with more than one valence state. Fluorine should be measured by EPMA (Valley et al., 1983). These assumptions are not met for hydrous minerals, e.g. amphiboles, micas, chlorites, hydro-garnets, and staurolites; because H_2O is not measured by EPMA (Essene, 1989). It is well known that charge balance does not yield a unique result when the assumptions fail (Droop, 1987) and we will not discuss these minerals. Instead we focus on the garnet group (excluding hydrous species where H_2O was unmeasured), where the authors believe charge-balance calculations to be a valuable tool after EPMA analysis.

Methods

We calculate $Fe^{3+}/\sum Fe$ by charge-balance for garnets (Table 1) according to the following procedure:

1) calculate the formula from EPMA data normalized to 8 cations;

2) calculate the total charge contribution from all cations assuming all *Fe* is Fe^{2+};

3) a) if the total cation charge is greater than 24 (cation charge of an ideal formula), then all *Fe* is ferrous and there is no ferric *Fe*;

b) if the cation charge is less than 24, calculate the amount of Fe^{3+} cations by subtracting the total cation charge from 24, i.e.

$$Fe^{3+} = 24 - \sum_i C_i V_i \qquad \text{(Eqn. 1)}$$

where C is the amount of the i th cation and V is the valence of the i th cation;

4) a) if the amount of calculated Fe^{3+} is greater than total *Fe*, then enter zero for Fe^{2+} and set Fe^{3+} to equal total *Fe*,

b) if the amount of calculated Fe^{3+} is less than total *Fe*, subtract the calculated Fe^{3+} from the total *Fe* to determine amount of Fe^{2+}.

This procedure is slightly different than that of Droop (1987), but is preferred by the authors due to its simplicity. For each data set we back-calculated total *Fe* as *FeO* from reported *FeO* and/or Fe_2O_3 and the above procedure was implemented to ensure consistency of charge balance calculations. If data for H_2O, Li_2O, or other oxides that are not typically measured by EPMA are available through another method e.g. secondary ion mass spectrometry (Schingaro et al., 2016) or Fourier transform infrared spectroscopy (Locock et al., 1995), then they can be combined with EPMA data and incorporated into charge balance calculations according to Grew et al. (2013).

The accuracy of charge-balance calculations is dependent on several factors. Counting statistics during EPMA analysis provides an assessment of instrumental precision, but not of accuracy. Choice of analytical standards can make critical differences for EPMA of silicates and oxides, including garnets due to chemical peak shifts for Mg- and Al-Kα between non-garnet standards and sample garnets (Fournelle, 2007; Fournelle and Jonnard, 2011). Fournelle and

Geiger (2010) examined EPMA of synthetic grossular and pyrope, using non-garnet standards (e.g. wollastonite, corundum, Fo-rich olivine) and noted a range of errors (Al – 3% low; Mg – 1% high; Si – 1% high) and different possible analytical results that were dependent upon (1) which mass absorption coefficient and (2) which matrix correction were used. These results emphasize the need for garnets as standards, ideally for all elements, obviating any chemical peak shift and minimizing error in matrix correction.

Conditions of EPMA analysis and the selected standards, mass absorption coefficients, and matrix correction are not always reported resulting in data that are difficult to evaluate (e.g. Li et al., 2005). Due to the vague nature of some reports, we estimate error bars by conducting a sensitivity analysis of $Fe^{3+}/\sum Fe$ to SiO_2. Data for Si are predicted to be the largest contribution to uncertainty in charge balance calculations because Si^{4+} is the most abundant cation and has the highest charge. For each sample, SiO_2 was adjusted by ± 1%, then $Fe^{3+}/\sum Fe$ was calculated by charge-balance and these values were used as endpoints for the error bars along the x-axis (Fig. 1). Note that in some cases the error bars are asymmetrical due to the fact that $Fe^{3+}/\sum Fe$ can not be less than 0 or greater than 1. If calculation of $Fe^{3+}/\sum Fe$ after propagating both +1 and -1% SiO_2 result in a $Fe^{3+}/\sum Fe$ value less than 0 (or both are greater than 1), then no error bar is shown because they do not encompass possible solutions. The uncertainty of $Fe^{3+}/\sum Fe$ calculations varies with total Fe; at ~ 5 wt% FeO(total) error in $Fe^{3+}/\sum Fe$ is more than triple that of garnets where FeO(total) is greater than 15 wt% (Fig. 2).

Discussion

Several garnet studies have compared EPMA/charge-balance with other methods and in general imply that accuracy of $Fe^{3+}/\sum Fe$ determination by charge-balance is questionable

(McGuire et al., 1989; Dyar et al., 1993; Canil and O'Neill, 1996; Sobolev et al., 1999; Li et al., 2005; Dyar et al., 2012; Schingaro et al., 2016). Sobolev et al. (1999) state "*…there is no direct (1:1) correlation between the two sets of data"* in reference to charge-balance vs. Mössbauer, but base this on 4 data with $Fe^{3+}/\sum Fe$ less than 0.20. Canil and O'Neill (1996) point out that charge balance errors are different between mineral species and increase in the relative order: spinel < garnet < pyroxene, due to differing amounts of Fe and SiO_2. Spinel has the highest Fe content and no Si, which results in $Fe^{3+}/\sum Fe$ values that are identical (with similar precisions) between charge balance and Mössbauer (Canil and O'Neill, 1996).

In the Dyar et al. (2012) study, three samples (AHUN, G5183, and BBKG) showed particularly large differences in $Fe^{3+}/\sum Fe$ (up to 0.93 vs. 0.00) when derived from Mössbauer spectroscopy vs. when calculated by charge-balance (asterisks in Fig. 1). However, we have recalculated the data in Table 2 of Dyar et al. (2012) and found errors. These errors are acknowledged in an erratum (Dyar et al., 2016; this volume) where all *Fe* is reported as total iron converted to *FeO*. Dyar et al. (2016) also correct sample localities and/or mineral identifications for 5 garnets from the Adirondack Mountains, N.Y. that we pointed out as unlikely based on EPMA estimates of $Fe^{3+}/\sum Fe$. Our recalculated $Fe^{3+}/\sum Fe$ values are plotted as white squares (Fig. 1). After recalculation, samples AHUN, G5183, and BBKG show greatly improved agreement between the EPMA/charge-balance and Mössbauer spectroscopic methods (Fig. 1). The difference in $Fe^{3+}/\sum Fe$ between the charge-balance and Mössbauer methods for the recalculated dataset is on average 0.06 and the largest is 0.38 (Table 1; Fig 1). To our knowledge, none of the EPMA data employed garnet standards and we predict that the agreement in Fig. 1 could be enhanced if good garnet standards are developed.

Several studies measure $Fe^{3+}/\sum Fe$ in natural garnet by Mössbauer and report EPMA data, but do not calculate $Fe^{3+}/\sum Fe$ by charge-balance (Kühberger et al.; Locock et al., 1995; McCammon et al., 1998; Chakhmouradian and McCammon, 2005). Many other M˜ssbauer studies of $Fe^{3+}/\sum Fe$ in garnets exist, but mostly investigate synthetic rare-earth-element garnets (e.g. yttrium-aluminum-garnet), which are considerably different than natural garnets and are not compared here. We have calculated $Fe^{3+}/\sum Fe$ from the natural garnets using reported EPMA values (in some cases back calculating total Fe from FeO and Fe_2O_3) and compare the results to their reported M˜ssbauer determinations of $Fe^{3+}/\sum Fe$ (Fig. 1). For this suite of garnets there is a general 1:1 correlation between charge-balance and Mössbauer spectroscopy.

There is no reason to expect charge-balance to be more accurate than Mössbauer spectroscopy. However, if Mössbauer (or a comparable technique) is not available, then charge-balance calculations are a significant improvement over assuming all Fe to be ferric or ferrous.

Implications

We conclude that $Fe^{3+}/\sum Fe$ estimates in garnet by charge-balance from high-quality EPMA data provide a suitable alternative to direct measurement of $Fe^{3+}/\sum Fe$ when Mössbauer spectroscopy or other comparable techniques are not practical, particularly for Fe-rich species such as almandine and andradite. These results support the utility of charge balance calculations for other anhydrous minerals that meet the criteria described here for garnets.

References cited

Bajt, S., Sutton, S., and Delaney, J., 1994. X-ray microprobe analysis of iron oxidation states in silicates and oxides using X-ray absorption near edge structure (XANES). Geochimica et Cosmochimica Acta, **58**, 5209-5214.

Canil, D., and O'Neill, H.S.C., 1996. Distribution of ferric iron in some upper-mantle assemblages. Journal of Petrology, **37**, 609-635.

Chakhmouradian, A., and McCammon, C., 2005. Schorlomite: a discussion of the crystal chemistry, formula, and inter-species boundaries. Physics and Chemistry of Minerals, **32**, 277-289.

Droop, G.T.R., 1987. A gneral equation for estimating Fe3+ concentrations in ferromagnesian silicates and oxides from microprobe analyses, using stoichiometric criteria. Mineralogical Magazine, **51**, 431-435.

Dyar, M.D., Agresti, D.G., Schaefer, M.W., Grant, C.A., and Sklute, E.C., 2006. Mössbauer spectroscopy of earth and planetary materials. Annu. Rev. Earth Planet. Sci., **34**, 83-125.

Dyar, M.D., Breves, E.A., Emerson, E., Bell, S.W., Nelms, M., Ozanne, M.V., Peel, S.E., Carmosino, M.L., Tucker, J.M., Gunter, M.E., Delaney, J.S., Lanzirotti, A., and Woodland, A.B., 2012. Accurate determination of ferric iron in garnets by bulk Mossbauer spectroscopy and synchrotron micro-XANES. American Mineralogist, **97**, 1726-1740.

Dyar, M.D., Breves, E.A., Emerson, E., Bell, S.W., Nelms, M., Ozanne, M.V., Peel, S.E., Carmosino, M.L., Tucker, J.M., Gunter, M.E., Delaney, J.S., Lanzirotti, A., and Woodland, A.B., 2016. Erratum: Accurate determination of ferric iron in garnets by bulk Mössbauer and synchrotron micro-XANES spectroscopies. American Mineralogist, **101**, xxx.

Dyar, M.D., Guidorttri, C.V., Holdaway, M.J., and CoLucci, M., 1993. Nonstoichiometric hydrogen contents in common rock-forming hydroxyl silicates. Geochimica et Cosmochimica Acta, **57**, 2913-2918.

Essene, E., 1989. The current status of thermobarometry in metamorphic rocks. Geological Society, London, Special Publications, **43**, 1-44.

Fournelle, J., Peak Shifts in Al, Mg, Si and Na Ka in Geologically Important Materials, in Proceedings AGU Fall Meeting Abstracts2007, Volume 1, p. 0328.

Fournelle, J., and Geiger, C., An electron microprobe study of synthetic aluminosilicate garnets, in Proceedings American Geophysical Union, Fall Meeting 2010, abstract V51C□22082010.

Fournelle, J., and Jonnard, P., Peak Shift in Mg Ka in EPMA: High Resolution X-ray Spectrometer Results for Silicate and Oxide Minerals, in Proceedings AGU Fall Meeting Abstracts2011, Volume 1, p. 2542.

Garvie, L.A., and Buseck, P.R., 1998. Ratios of ferrous to ferric iron from nanometre-sized areas in minerals. Nature, **396**, 667-670.

Grew, E.S., Locock, A.J., Mills, S.J., Galuskina, I.O., Galuskin, E.V., and Hålenius, U., 2013. Nomenclature of the garnet supergroup. American Mineralogist, **98**, 785-811.

Höfer, H.E., and Brey, G.P., 2007. The iron oxidation state of garnet by electron microprobe: Its determination with the flank method combined with major-element analysis. American Mineralogist, **92**, 873-885.

Johnson, W.M., and Maxwell, J.A., 1981, Rock and mineral analysis, John Wiley & Sons.

Kühberger, A., Fehr, T., Huckenholz, H.G., and Amthauer, G., Crystal chemistry of a natural schorlomite and Ti-andradites synthesized at different oxygen fugacities. Physics and Chemistry of Minerals, **16**, 734-740.

Lalonde, A., Rancourt, D., and Ping, J., 1998. Accuracy of ferric/ferrous determinations in micas: a comparison of Mössbauer spectroscopy and the Pratt and Wilson wet-chemical methods. Hyperfine interactions, **117**, 175-204.

Li, Y.-L., Zheng, Y.-F., and Fu, B., 2005. Mössbauer spectroscopy of omphacite and garnet pairs from eclogites: Application to geothermobarometry. American Mineralogist, **90**, 90-100.

Locock, A., Luth, R.W., Cavel, R.G., Smith, D.G., Duke, M., and John, M., 1995. Spectroscopy of the cation distribution in the schorlomite species of garnet. American Mineralogist, **80**, 27-38.

McCammon, C., Chinn, I., Gurney, J., and McCallum, M., 1998. Ferric iron content of mineral inclusions in diamonds from George Creek, Colorado determined using Mössbauer spectroscopy. Contributions to Mineralogy and Petrology, **133**, 30-37.

McGuire, A.V., Dyar, M.D., and Ward, K.A., 1989. Neglected Fe^{3+}/Fe^{2+} ratios—A study of Fe^{3+} content of megacrysts from alkali basalts. Geology, **17**, 687-690.

Raeburn, S.P., Ilton, E.S., and Veblen, D.R., 1997a. Quantitative determination of the oxidation state of iron in biotite using X-ray photoelectron spectroscopy: I. Calibration. Geochimica et Cosmochimica Acta, **61**, 4519-4530.

Raeburn, S.P., Ilton, E.S., and Veblen, D.R., 1997b. Quantitative determination of the oxidation state of iron in biotite using X-ray photoelectron spectroscopy: II. In situ analyses. Geochimica et Cosmochimica Acta, **61**, 4531-4537.

Schingaro, E., Lacalamita, M., Mesto, E., Ventruti, G., Pedrazzi, G., Ottolini, L., and Scordari, F., 2016. Crystal chemistry and light elements analysis of Ti-rich garnets. American Mineralogist, **101**, 371-384.

Schmid, R., Wilke, M., Oberhänsli, R., Janssens, K., Falkenberg, G., Franz, L., and Gaab, A., 2003. Micro-XANES determination of ferric iron and its application in thermobarometry. Lithos, **70**, 381-392.

Sobolev, V.N., McCammon, C.A., Taylor, L.A., Snyder, G.A., and Sobolev, N.V., 1999. Precise Mössbauer milliprobe determination of ferric iron in rock-forming minerals and limitations of electron microprobe analysis. American Mineralogist, **84**, 78-85.

Valley, J., Essene, E., and Peacor, D., 1983. Fluorine-bearing garnets in Adirondack calc-silicates. American Mineralogist, **68**, 444-448.

Wilson, A., 1960. The micro-determination of ferrous iron in silicate minerals by a volumetric and a colorimetric method. Analyst, **85**, 823-827.

Figure and Table captions:

Figure 1. Comparison of $Fe^{3+}/\sum Fe$ ratios in garnets derived from electron probe microanalysis (EPMA) and charge-balance vs. Mössbauer spectroscopy (MS). The error bar size was calculated by propagating ± 1% of the SiO_2 wt% value through charge balance calculations. Two data with error bar width of 0 result from the constriction that $Fe^{3+}/\sum Fe$ can not be negative or greater than 1. If both the maximum and minimum ends of the error bar calculation are less than 0 or greater then 1, an error bar of width = 0 results. Error bars for MS values are approximately the size of the data points (± 0.01). The $Fe^{3+}/\sum Fe$ cation ratios

calculated from the oxide data in Table 2 of Dyar et al. (2012; “reported”) are compared to the recalculated values in Table 1. Samples AHUN, G5183 and BBKG are labeled.

Figure 2. Correlation between $Fe^{3+}/\sum Fe$ error and wt% total Fe in garnets. The magnitude of error in $Fe^{3+}/\sum Fe$ calculations (y-axis values) were calculated by propagating ± 1% of the SiO_2 wt% value through charge balance calculations. Two data with error bar width of 0 (i.e. y = 0) result from the constriction that $Fe^{3+}/\sum Fe$ can not be negative or greater than 1. If both the maximum and minimum ends of the error bar calculation are less than 0 or greater then 1, an error bar of width = 0 results.

Table 1. Comparison of $Fe^{3+}/\sum Fe$ determined by electron probe microanalysis (EPMA) and charge-balance vs. Mössbauer spectroscopy (MS).

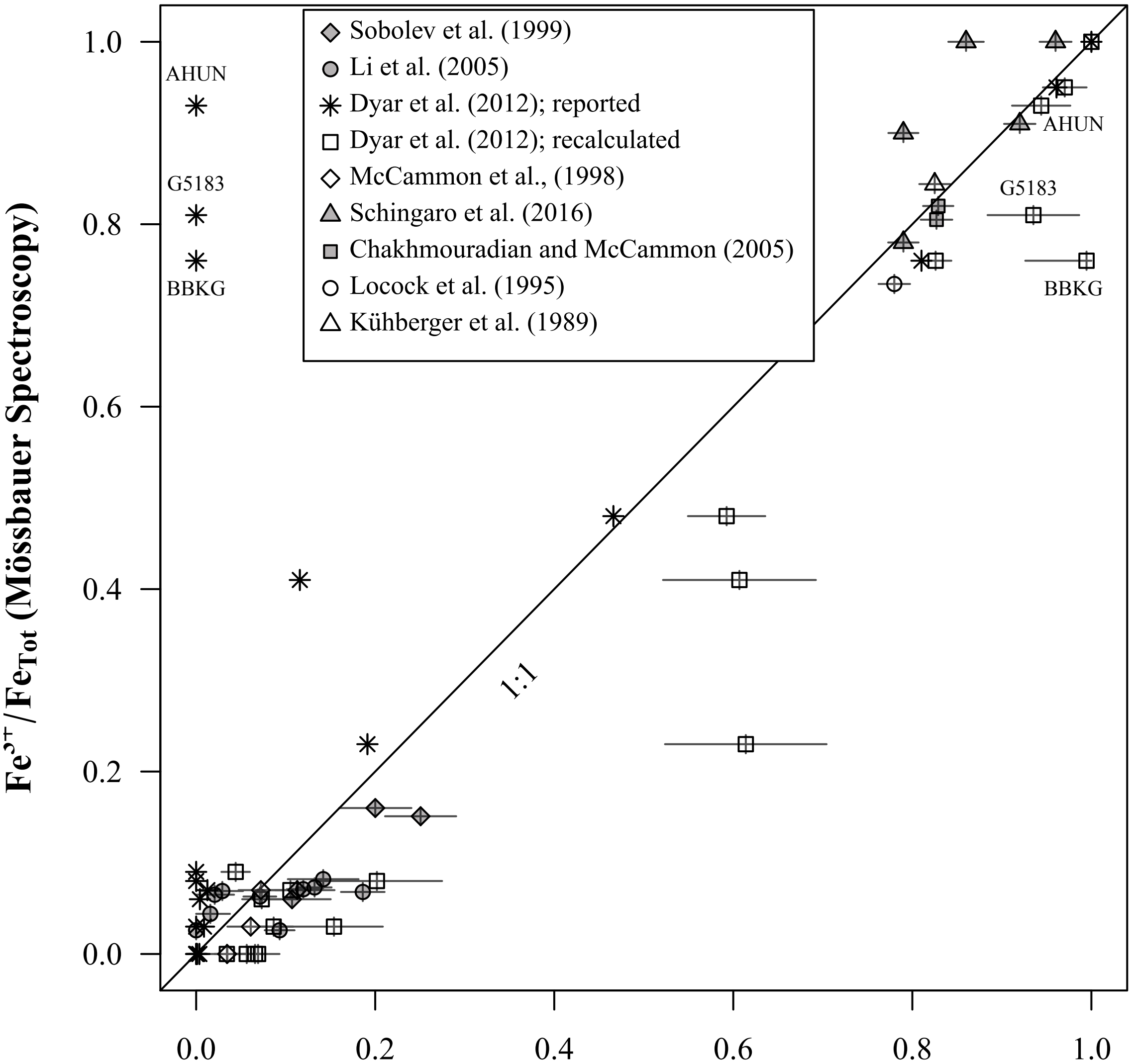

◆ Sobolev et al. (1999)
● Li et al. (2005)
✳ Dyar et al. (2012); reported
□ Dyar et al. (2012); recalculated
◇ McCammon et al., (1998)
▲ Schingaro et al. (2016)
■ Chakhmouradian and McCammon (2005)
○ Locock et al. (1995)
△ Kühberger et al. (1989)
AHUN
G5183
BBKG
AHUN
G5183
BBKG
1:1
1.0
0.8
0.6
0.4
0.2
0.0
0.0
0.2
0.4
0.6
0.8
1.0
Fe^{3+}/Fe_{Tot} (Mössbauer Spectroscopy)
Fe^{3+}/Fe_{Tot} (Charge Balance)

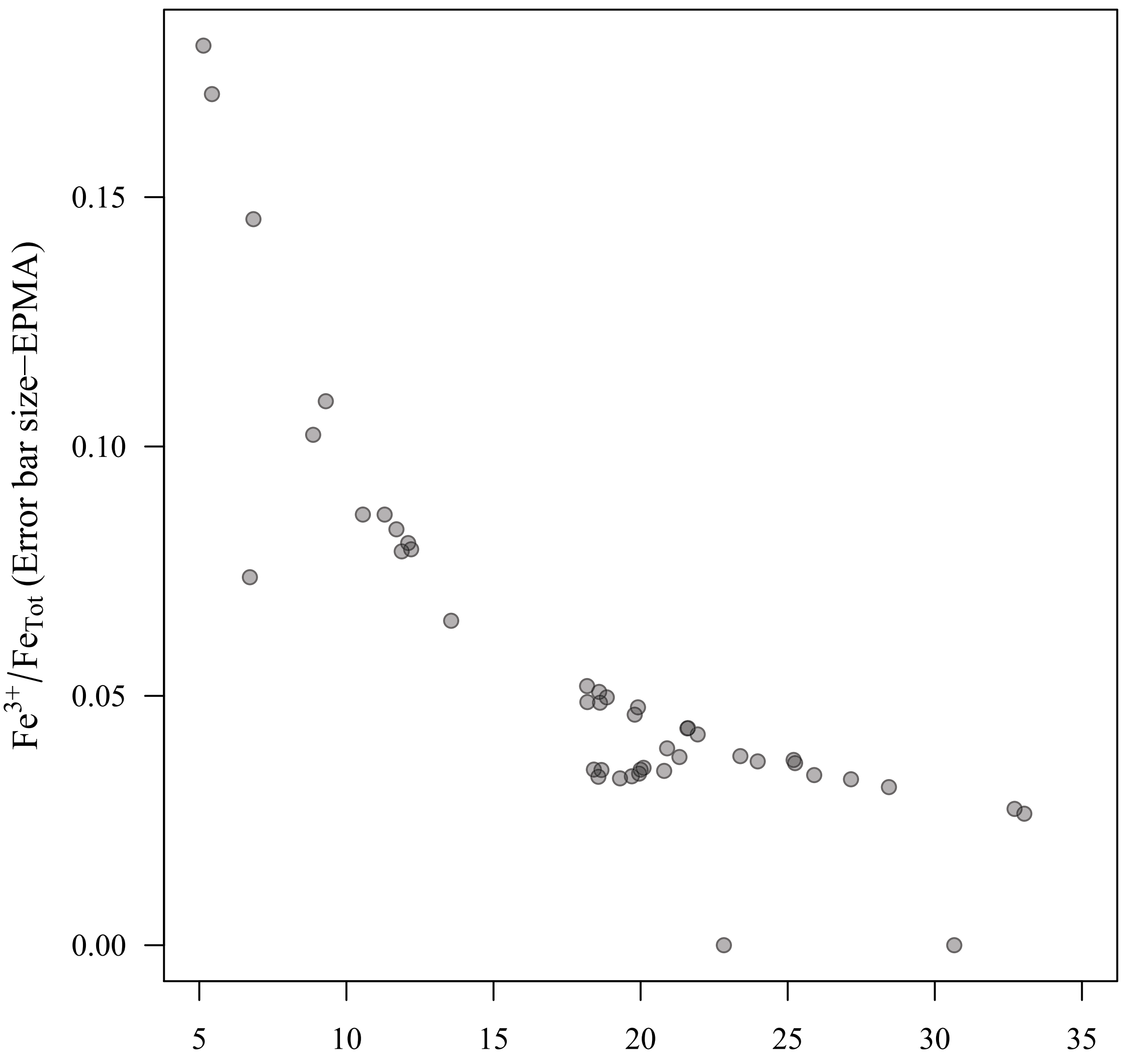
Fe^{3+}/Fe_{Tot} (Error bar size−EPMA)
0.00
0.05
0.10
0.15
5
10
15
20
25
30
35
Total Fe as FeO (Wt%)

Table 1: Comparison of $Fe^{3+}/\sum Fe$ determined by electron probe microanalysis (EPMA) and charge-balance vs. Mössbauer spectroscopy (MS).

Sample	SiO_2 (wt%)	Total Fe as FeO (wt%)	$Fe^{3+}/\sum(Fe)$ (EPMA) [a]	$Fe^{3+}/\sum Fe$ (MS)	$Fe^{3+}/\sum(Fe)$ diff. (EPMA-MS)	Reference
236-4	40.39	11.30	0.11	0.06	0.05	Sobolev et al. (1999)
237-2	40.39	11.70	0.11	0.07	0.04	Sobolev et al. (1999)
281-2	40.39	12.10	0.20	0.16	0.04	Sobolev et al. (1999)
281-4	40.10	12.20	0.25	0.15	0.10	Sobolev et al. (1999)
97h03	38.16	25.25	0.07	0.06	0.01	Li et al. (2005)
97h06	39.34	22.83	0.00	0.03	-0.03	Li et al. (2005)
97h32	37.39	27.15	0.09	0.03	0.07	Li et al. (2005)
94m44	38.66	21.32	0.02	0.04	-0.03	Li et al. (2005)
94m55	39.15	21.94	0.02	0.07	-0.04	Li et al. (2005)
94m67	37.90	19.80	0.03	0.07	-0.04	Li et al. (2005)
94m80	36.59	23.98	0.12	0.07	0.05	Li et al. (2005)
944010-2	37.48	18.62	0.19	0.07	0.12	Li et al. (2005)
944012-11	38.84	11.88	0.14	0.08	0.06	Li et al. (2005)
97m30	36.71	23.39	0.13	0.07	0.06	Li et al. (2005)
A32W	38.05	6.72	0.99	0.76	0.23	Dyar et al. (2012)
9710	37.32	28.44	0.04	0.09	-0.05	Dyar et al. (2012)
9723	36.58	25.90	0.11	0.07	0.04	Dyar et al. (2012)
9729	36.07	33.04	0.07	0.00	0.07	Dyar et al. (2012)
2A	39.31	19.91	0.07	0.00	0.07	Dyar et al. (2012)
2B	38.86	21.59	0.07	0.06	0.01	Dyar et al. (2012)
8A	38.75	25.20	0.06	0.00	0.06	Dyar et al. (2012)
9B	37.75	10.56	0.59	0.48	0.11	Dyar et al. (2012)
HE1	38.95	21.61	0.09	0.03	0.06	Dyar et al. (2012)
HRM1	36.71	18.19	0.97	0.95	0.02	Dyar et al. (2012)
AHUN	36.52	13.56	0.94	0.93	0.01	Dyar et al. (2012)
G5183	37.58	8.87	0.94	0.81	0.13	Dyar et al. (2012)
ALM	37.01	32.71	0.03	0.00	0.03	Dyar et al. (2012)
G89	38.36	5.43	0.61	0.41	0.20	Dyar et al. (2012)
G17	38.38	5.14	0.61	0.23	0.38	Dyar et al. (2012)
AND	34.52	30.66	1.00	1.00	0.00	Dyar et al. (2012)
1251	41.22	6.84	0.20	0.08	0.12	Dyar et al. (2012)
129	42.00	9.30	0.15	0.03	0.12	Dyar et al. (2012)
BBKG	29.14	20.00	0.83	0.76	0.07	Dyar et al. (2012)
7	39.09	18.59	0.03	0.00	0.03	McCammon et al. (1998)
20	39.11	18.18	0.06	0.03	0.03	McCammon et al. (1998)
55	38.78	18.85	0.07	0.07	0.00	McCammon et al. (1998)
w6	26.73	19.30	0.79	0.90	-0.11	Schingaro et al. (2016)
w12	29.60	20.10	0.96	1.00	-0.04	Schingaro et al. (2016)
w16	27.62	19.70	0.79	0.78	0.01	Schingaro et al. (2016)
nzala	30.10	20.80	0.92	0.91	0.01	Schingaro et al. (2016)
zer2	34.16	20.90	0.86	1.00	-0.14	Schingaro et al. (2016)
AF-05	26.84	18.41	0.83	0.81	0.02	Chakhmouradian & McCammon (2005)
MC-04	25.96	18.56	0.83	0.82	0.01	Chakhmouradian & McCammon (2005)
Ice River Schorlomite	27.15	18.67	0.78	0.73	0.05	Locock et al. (1995)
Schorlomite	28.41	19.95	0.82	0.84	-0.02	Kühberger et al. (1989)

[a] Ratio calculated based on charge-balance calculations.